

Charge ordering and inter-layer coupling in cuprates

P. Sule

Research Institute for Technical Physics and Material Science,
Konkoly Thege u. 29-33, Budapest, Hungary,
sule@mf.kfki.hu

(September 28, 2024)

The inter-layer direct Coulomb coupling is analyzed in a charge ordered superlattice bilayer model in which pairing is supported by inter-layer Coulomb energy gain (potential energy driven superconductivity). The 2D pair-condensate can be characterized by a charge ordered state with a "checkerboard" like pattern seen by scanning tunneling microscopy. The 2D, 3D quantum phase transition of the hole-content at T_c , supported by c-axis optical measurements, is also studied. The pair condensation might lead to the sharp decrease of the normal state c-axis anisotropy of the hole content and hence to the decrease of inter-layer dielectric screening. The drop of the c-axis dielectric screening can be the primary source of the condensation energy below T_c . We find that a net gain in the electrostatic energy occurs along the c-axis, which is proportional to the measured condensation energy (U_0) and with $T_c: E_c^{3D} = 2(a_b/a_0 + 1)^2 U_0$ for T_c and is due to inter-layer charge complementarity (charge asymmetry of the boson condensate) where a_b is the coherence length of the condensate and $a_0 \approx 3.9\text{\AA}$ is the in-plane lattice constant. The model naturally leads to the effective mass of $m \approx 4m_e$ found by experiment. The static c-axis dielectric constant ϵ_c is calculated for various cuprates and compared with the available experimental data. We find correlation between T_c and the inter-layer spacing d_c and with the coherence area of the condensate.

PACS numbers: 74.20.-z, 74.25.-q, 74.72.-h

I. INTRODUCTION

It is more or less generally accepted now that the conventional electron-phonon pairing mechanism cannot explain cuprate superconductivity, because as high a transition temperature as 164K (the record T_c up to now [1]) cannot be explained by the energy scale of lattice vibrations without leading to lattice instability [2]. It is already well established that much of the physics related to high-temperature superconductivity (HTSC) is in 2D nature, one of the basic questions to be answered, however, in the future is whether HTSC is a strictly 2D phenomenon or should also be described by a 3D theory.

A well known experimental fact is that the zero resistance occurs along the ab plane and the c-axis at the same critical temperature [3] suggesting that there must be inter-layer (IL) coupling involved in the mechanism which drives the system into HTSC. Another experiment, such as the intercalation on Bi_2Te_2 [4], however leads to the opposite conclusion. Intercalation of I or organic molecules, which expands the unit cell significantly along the c-axis, does not affect T_c . This finding is against IL coupling and supports low-dimensional theories. The large anisotropy of the resistivity (and of other transport properties) is again not in favour of 3D theories of HTSC [3].

Experiments on $\text{YBa}_2\text{Cu}_3\text{O}_{7-y}$ (YBCO) ultrathin artificial HTSC compounds, sandwiched between thick non-superconducting $\text{PbBa}_2\text{Cu}_3\text{O}_{7-y}$ (PBCO) layers [3,5] and measurements on $(\text{BaCuO}_{2+x})_2 = (\text{CaCuO}_2)_n$ heterostructures [6] indicate the continuous decrease of

T_c with the decreasing number of superconducting (SC) layers. In particular the one-unit-cell thick sample of YBCO/PBCO heterostructure exhibits $T_c \approx 20\text{ K}$ [5,7]. Other heterostructures, such as the $(\text{Ba}_{0.9}\text{Nd}_{0.1}\text{CuO}_{2+x})_5 = (\text{CaCuO}_2)_2 = (\text{Ba}_{0.9}\text{Nd}_{0.1}\text{CuO}_{2+x})_5$, containing a single bilayer SC block isolated from each other by insulating blocks, were shown to have $T_c \approx 55\text{ K}$ [8]. These findings again indicate the importance of IL coupling in high temperature superconductors. There are a couple of other findings against and supporting the 3D nature of HTSC [9-11]. Most notably the systematic dependence of the transition temperature T_c on the c-axis structure and, in particular, on the number of CuO_2 planes in multilayer blocks are also strongly in favour of the 3D character of HTSC. It is therefore, a fundamental question whether at least a weak IL coupling is needed for driving the system to a superconducting (SC) state or a single CuO_2 layer is sufficient for HTSC [12].

There has been considerable effort spent on understanding HTSC within the context of IL coupling mechanism in the last decades in which c-axis energy is available as a pairing mechanism [13-16]. In other approaches the importance of IL hopping is emphasized vs. the direct IL Coulomb interaction of charged sheets [9,12]. There is another theory providing explanation for HTSC using the general framework of BCS combined with IL coupling [17]. The so-called IL tunnelling (ILT) theory [9,12], however, is no longer considered a viable mechanism for SC in cuprates since ILT could provide no more than 1% of the condensation energy in certain cuprates [2,10,18].

In this paper we propose a simple phenomenologi-

cal model for explaining the 3D character of HTSC in cuprates supported by calculations. We would like to study the magnitude of direct Coulomb interaction between charge ordered square superlattice layers as a possible source of pairing interaction. Our intention is to understand HTSC within the context of an IL Coulomb-mediated mechanism. Of particular relevance to our investigation are the doping, multilayer, and pressure dependence of T_c in terms of a charge ordered superlattice nature of pair condensation.

The size of a charge ordered characteristic superlattice can directly be related to the in-plane coherence length a_{ab} of cuprates, which is proportional to the linear size of the pair condensate (real space pairing) in the ab-plane [19]. The relevant length scale for superconductors is the characteristic size of the Cooper-pair and can be estimated by an uncertainty-principle argument [19]. Only those charge carriers play a decisive role in HTSC which has energy within $k_B T_c$ of the Fermi energy and sets in at T_c with the momentum range $p \sim k_B T_c/v_F$, where v_F is the Fermi velocity, leading to the definition of the Pippard's characteristic length [19]

$$a_{ab} \sim \frac{h v_F}{k_B T_c} \quad (1)$$

where a is a numerical constant of order unity, to be determined. a_{ab} is a relevant number for describing the 2D confinement of the pair-condensate wave function below T_c . a_{ab} can also directly be obtained according to the anisotropic Ginsburg-Landau theory via the measurement of the upper critical field $H_{c2,ab}$ [19]. It has been shown recently that a_{ab} obtained from Eq. (1) or from $H_{c2,ab}$ measurements are very close to each other [20].

The IL charging energy we wish to calculate depends then on the IL spacing (d), the IL dielectric constant ϵ_c , the hole content p and the size of the superlattice. A large body of experimental data are collected which support our model. A consistent picture is emerged on the basis of the careful analysis of this data set. Finally we calculate the static c-axis dielectric constant ϵ_c for various cuprates which are compared with the available experimental observations.

II. OPTIMAL DOPING AND THE 2D-3D PHASE TRANSITION OF THE HOLE-CONTENT

It is commonly accepted that charge carriers are mainly confined to the 2D CuO_2 layers and their concentration is strongly influenced by the doping agent via hole doping. Holes (no charge and spin at a lattice site) in the 2D CuO_2 layers are the key superconducting elements in high temperature superconductivity (HTSC). A characteristic feature of many high temperature superconductors (HTSCs) is the optimal hole content value of $p_0 \approx 0.16$ per CuO_2 layer at optimal doping measured in the normal state (NS) [21]. This general feature of

cuprates can be summarized in the parabolic dependence of the maximum critical temperature T_c^m ,

$$T_c = T_c^m = 1.825(p - p_0)^2; \quad (2)$$

where T_c^m corresponds to the optimal hole concentration p_0 [22]. Since T_c appears to be maximized at $p_0 \approx 0.16$, we pay special attention to the IL Coulomb interaction in cuprates at this particular hole concentration.

Our starting hypothesis is that the hole content goes through a reversible 2D, 3D quantum phase transition at T_c in layered copper oxides. Optical studies on the c-axis charge dynamics reveals this phenomenon: the c-axis resistance is nearly insulating in the NS but below T_c is dominated by the Josephson-like plasma edge [23]. Below T_c a sharp reflectivity edge is found at very low frequencies (lower than the superconducting gap) for a variety of cuprates arising from the carriers condensed in the SC state to the ab-plane and due to the onset of a coherent charge transport along the c-axis [24-28]. The appearance of plasma in the SC state and the absence of it in the NS seem to be a common feature of HTSC cuprates [27]. Band structure calculations predict an appreciable c-axis dispersion of bands close to the Fermi surface and thus an anisotropic three-dimensional metallic state [29]. Other first principles calculations indicate that above T_c the hole charge p is charge transferred to the doping site in the charge reservoir (2D \rightarrow 3D transition) [30,31].

Furthermore, we expect that below T_c the hole-content is condensed to the sheets forming anti-hole regions (hole-content charge at a lattice site, 3D \rightarrow 2D transition). An anti-hole corresponds to an excess charge condensed to a hole lattice site in the sheets below T_c . Therefore, in the normal state hole doping is the dominant charge transfer mechanism while in the superconducting (SC) state the opposite is true: the IL hole-charge is transferred back to the CuO_2 planes (charging of the sheets). The latter mechanism can be seen by the measurement of transport properties as a function of temperature [3,32-34] if we assume that the increase in the density of in-plane free carriers below T_c is due to pair condensation. The sharp temperature dependence of the c-axis dielectric constant ϵ_c and optical conductivity [35] seen in many cuprates and in other perovskite materials also raises the possibility of a 2D, 3D charge density condensation mechanism at T_c [3,38]. Therefore, the pair condensation can be described by an anisotropic 3D condensation mechanism, and by a doping induced 2D-3D dimensional crossover [11].

In any naive model of electron pairing in cuprates the Coulomb repulsion is troublesome. When the pairs of charged carriers are confined to the sheets, naturally a net self-repulsion of the pair condensate occurs. Although short-range Coulomb screening in the dielectric crystal can reduce the magnitude of the repulsion but it is insufficient to cancel Coulomb repulsion [39]. Spatial separation should reduce the interaction strength, but even at 14 \AA $e^2/r \approx 1 \text{ eV}$ if unscreened. One can assume capacitive effect between the CuO_2 planes: The

charged boson condensate in one plane is stabilized by a deficiency of that charge on another plane [39]. The various forms of the capacitor model are associated with the 3D character of HTSC, considering the inter-layer charge reservoir as a dielectric medium [39]. The inter-layer charging energy might be insufficient to stabilize the self-repulsion of the holes in one plane and the self-repulsion of the charge condensate on another plane in the capacitor model. Also, the superconducting properties of the hole-rich and nearly hole-free sheets would be different which is not verified by experimental techniques.

Our intention is to combine the 2D and 3D nature of HTSC. Therefore, we propose a phenomenological model in which the charge distribution of the planes is polarized in such a way that holes and anti-holes (hole-electron pair) are phase separated within each of the sheets leading to a charge ordered state (COS). Recently, signatures of charge ordering have been found in various cuprates and manganites in the presence and the absence of magnetic fields [41-44]. Furthermore, the "checkerboard" charge pattern seen in Bi2212 [41] with spin periodicity of $\sim 8a_0$ strengthens our expectation that the SC state can be characterized by a COS. We focus on, then, the magnitude of IL coupling (direct IL Coulomb interaction) between 2D static charge ordered superlattices.

Charging of the sheets: The CuO_2 layers carry negative charge obtained from the charge reservoir even in the insulating stoichiometric materials, e.g. in the infinite layer compound CaCuO_2 each layer is charged by $2e$ charge donated by the Ca atoms. In $(\text{CuO}_2)^2$ then the electron configuration of Cu and O is $3d^0 4s^1$ and $2p_z^2$. Unit $(\text{CuO}_2)^2$ is typical of any undoped (stoichiometric) cuprates and ab initio calculations provide approximately the charge state $\text{Cu}^{1.5+} \text{O}_2^{3.5-}$ [3,29] which is due to charge redistribution between Cu and O. The $(\text{CuO}_2)^2$ plane itself is antiferromagnetic and insulating, e.g. there are no holes in the "overcharged" layers. Upon e.g. oxygen doping, however, the doping charge p is transferred along the c -axis to the doping site in the charge reservoir, since the doping atom exhibits a rare gas electron structure (O^{2-} , if oxygen doping) [30,31].

Briefly, the c -axis anisotropy of the hole content is strongly temperature dependent in cuprates. Our basic assumption is that in the SC state every second hole is filled up with the charge of $2p$ due to the condensation of the hole-content to the sheets leading to a charge ordered state in the SC state. Therefore the annihilation of the half of the holes results in the appearance of a hole-anti-hole pair. The hole-anti-hole pairs are the basic quasiparticles of the SC COS. The phase separation of the holes and anti-holes (leading to a charge ordered state) is stabilized by the intra- and inter-layer hole-anti-hole interactions. Basically the phase separation of holes and anti-holes in the planes is the manifestation of strong Coulomb correlation in the SC state. The superconducting charge-ordered states in cuprates are characterized theoretically based on the assumption that cuprates are in close proximity to quantum critical points where

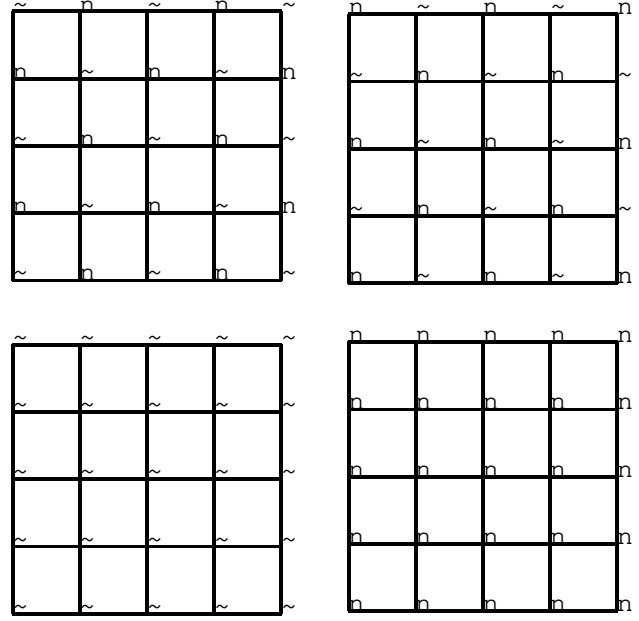


FIG. 1. Upper panels: The charge ordered state of the type of a "checkerboard" of the hole-anti-hole condensate. Open and filled circles denote the holes with a charge of $q_1 = +0.16e$ and anti-holes ($q_2 = -0.16e$), respectively in the $4a_0 \times 4a_0$ (5×5) square lattice layer model. Note that the left panel accommodates 13 anti-holes which corresponds to $2e + 0.16e = 2.16e$ charge. The right panel contains 12 anti-holes corresponding to $2e - 0.16e = 1.84e$ charge. The two lower panels correspond to the antiferromagnetic insulating state (left) and to a non charge ordered hole-doped system (normal state, right).

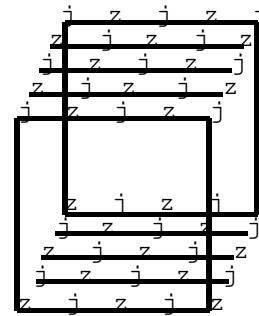


FIG. 2. The charge ordered state of the hole-anti-hole condensate in the $4a_0 \times 4a_0$ charge ordered bilayer superlattice model. Note the charge asymmetry between the adjacent layers. The bilayer can accommodate a pair of boson condensate ($4e$). Noteworthy that holes (empty circles) and anti-holes (filled circles) can be characterized by stripes along the diagonal lines. The inter-layer charge complementarity of these charge stripes is crucial for the inter-layer Coulomb energy gain.

spin/or static charge order occurs in the SC state [45]. In this paper we will focus on the Coulomb interaction between the charge ordered sheets screened by the IL dielectric media (charge reservoir). It will be immediately apparent from our analysis that net energy gain occurs due to the IL Coulomb interaction of the charge ordered layers when the hole-electron charge pattern is asymmetrically distributed in the adjacent layers (Fig. 2).

III. THE SUPERLATTICE MODEL: THE COHERENCE AREA

We propose to examine the following superlattice model of pair condensation: A pair of charge carriers ($2e$) can be distributed over $2 \times 0.16 = 12.5$ CuO_2 unit cells in a square lattice layer if the $2e$ pair is composed of the hole content $p_0 = 0.16$ CuO_2 at optimal doping. However, allowing the phase separation of hole-anti-hole pairs, every second unit cell is occupied by $0.16e$ (anti-hole), and the rest is empty (holes, $+0.16e$), therefore we have 25 unit cells for a condensed pair of charge carriers (Fig. 1., that is the unit lattice of the pair condensate in the 5×5 supercell model). Therefore, $2p_0 = 0.32e$ hole charge condenses to every second hole forming anti-hole sites. The 25 lattice sites provide the hole content of $25 \times 0.16e = 4e$ and therefore $2e$ excess charge in the anti-hole sites. In other words a Cooper wave-function can be distributed on a 5×5 superlattice with a node of

$0.16e$ in every anti-hole site. The remarkable feature is that the size of the 5×5 condensate (four lattice spacings, $4a_0 = 15.5\text{\AA}$) is comparable with the measured small coherence length ξ_{ab} of single-layer cuprates ($\xi_{ab} = 10\text{\AA}$ to 20\AA) [3,19,44,46]. ξ_{ab} can directly be related to the characteristic size of the wave-pocket of the local Cooper pair (coherence area) [3,19]. The charge ordered superlattice model can in principle be applied not only for $p_0 = 0.16e$ but also for the entire doping regime. The only difference what happens is that the charge nodes in the charge ordered state changes upon doping and consequently the inter-layer coupling scales with the anti-hole charges in the underdoped regime. In the overdoped regime, however, the situation is more difficult [51,57].

Our expectation is that the COS of the 5×5 model given in Fig. 1 can be an effective model state for describing the SC state. An important feature of this model is the charge separation dq in the charge ordered state, where $+0.16e$ and $-0.16e$ partial boson charges are localized alternatively ($dq = 0.32e$). The hopping of charge carriers from the anti-hole sites to the holes can reduce the magnitude of the charge separation dq leading to the extreme case when $dq = 0$ which is nothing else then the $(\text{CuO}_2)^2$ antiferromagnetic insulating state. Therefore characteristic quantity of the SC state dq is directly related to the hole-content seen in cuprates in the NS as a function of doping.

The hopping of antiholes in such a charge ordered lattice layer might lead to SC without considering any lat-

tice vibration effects when dq is in the optimal regime. The freezing of the COS leads to insulating Wigner crystal (the NS) [40]. Therefore the melting of the crystallized COS is required for SC [45]. HTSC can be characterized in this way as a competition between a liquid-crystal-like striped COS (SC) and a Wigner-crystal-like phase (NS) in a semiclassical theory of hole dynamics [40].

Below T_c the charged-ordered state becomes stable compared with the competing phase of the NS supported by IL charging energy. Holes and antiholes are placed in such a way in adjacent layers to maximize IL charging energy. Therefore, holes in one of the layers are always covered by antiholes in the other layer and vice versa (Fig. 2, inter-layer electrostatic complementarity, bilayer 5×5 ($4a_0 \times 4a_0$) model). An important feature is then that the boson condensate can be described by an inter-layer charge asymmetry. The IL coupling of the boson-boson pairs in the bilayer 5×5 model naturally suggests the effective mass of charge carriers $m = 4m_e$, as it was found by measurements [47,50]. In the next section we generalize the 5×5 model to represent a real space periodicity of $N \times N$ coherence area. The charge ordered state presented in this article can also be studied as a charge density wave (CDW) condensed on a superlattice. Using the CDW terminology one has approximately two CDW within a characteristic bilayer with an amplitude of $0.16e$. This system might not be insulating if we assume high rate of intersite hopping and low rate of IL hopping of the charge carriers. Then the charge ordered state is stabilized due to the attractive IL Coulomb interactions of asymmetrically condensed neighbouring CDWs.

We characterize the purely hole-doped NS as follows: In each sheet each CuO_2 units possess $p = +0.16e$ charge. The hole charge p is charge transferred to the charge reservoir (doping site) above T_c . In this model one can naively expect that the self-repulsion of a hole rich sheet can be quite large. In order to reduce the hole-hole self-repulsion of the sheets, a hopping of p charge between the adjacent hole sites would result in the reduction of the repulsion leading to a Wigner-crystal-like COS depicted on Fig. 3. As is well known, the hopping of certain amount of charge (p) between the holes leads to metallic conductance which is typical of hole-doped cuprates. This is the normal state (NS) of the cuprates. Due to the strong c-axis anisotropy of the hole content in the NS IL dielectric screening is large in this state because of the increase in the dynamic component of the IL dielectric permittivity (ϵ_c) and therefore the IL interaction energy vanishes, $E_c^{NS} = 0$. That is the enhanced dielectric screening in the NS due to the localization of the hole content in the charge reservoir. The lack of the IL plasma edge in the c-axis optical spectra of various cuprates in the NS is a strong evidence of this phenomenon [60].

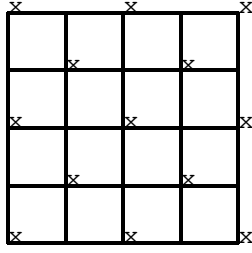


FIG. 3. A possible charge ordered state of the normal state. Opened and filled circles denote the holes with a charge of $q_h = +0.32e$ and antiholes ($q_a = -0.16e$), respectively in the 5×5 square lattice layer model.

Our proposal is to understand HTSC in such a way that the pair-condensate is stabilized at higher temperature by the IL-charging energy provided by the antisymmetry of the pair-condensate charge density between the adjacent layers. The c -axis dielectric constant of the SC state is reduced to the average value of the IL dielectric medium due to the pair condensation of the hole charge to the sheets. No IL screening of the hole charge occurs in this state which may well lead to energy gain.

IV. THE TOTAL ENERGY OF THE PAIR CONDENSATE

Our intention is to develop a simple working hypothesis in which the IL charge reservoir provides an average dielectric background and the hole content further enhances IL dielectric screening when $2D \rightarrow 3D$ transition occurs (hole-doping, the NS). The dielectric plasma provided by the hole charge results in the dynamic screening effect of Coulomb interaction which is typical of hole doped cuprates in the NS. In the opposite case ($3D \rightarrow 2D$, pair condensation) the IL dielectric screening is nearly reduced to the average background value of the IL ion core spacer. This is what leads to IL energy gain. The underlying source of the condensation energy is then the energy gain due to the lack of dynamic screening in the SC state. The possibility of direct IL hopping of Cooper pairs is not considered within this model as it was ruled out as important aspect of HTSC [10].

We start from a very general description of our model system using e.g. a Hamiltonian similar to that is given elsewhere [14] or which can also partly be seen in general text books [58]. We would like to describe then the $2D$, $3D$ condensation of the hole-content using the Hamiltonian

$$H = \sum_i \sum_{\sigma} H_i^{2D} + \sum_{i,j} H_{ij}^{3D}; \quad (3)$$

where H_i^{2D} is the BCS-type Hamiltonian of the intra-layer condensate.

$$H_i^{2D} = \sum_{\mathbf{k}} \sum_{\sigma} \epsilon_{\mathbf{k}} c_{\mathbf{k},i}^{\sigma\dagger} c_{\mathbf{k},i}^{\sigma} + V \sum_{\mathbf{k},\mathbf{k}'} \sum_{\sigma} c_{\mathbf{k},i}^{\sigma\dagger} c_{\mathbf{k}',i}^{\sigma} c_{\mathbf{k},i}^{\sigma} c_{\mathbf{k}',i}^{\sigma} \quad (4)$$

In Eq. (4) $c_{\mathbf{k},i}^{\sigma\dagger}$ is the creation operator for electrons in the i th layer, with linear momentum \mathbf{k} within the layer and spin σ , using the effective-mass approximation $\epsilon_{\mathbf{k}} = \hbar^2 \mathbf{k}^2 / 2m$. $V = -J$ is the attractive inter-layer interaction ($3D$ coupling) and is assumed to originate from some of the proposed mechanisms [9,13,15]. The attractive IL term H_{ij}^{3D} given by

$$H_{ij}^{3D} = \sum_{\mathbf{k},\mathbf{k}'} t \sum_{\sigma} c_{\mathbf{k},i}^{\sigma\dagger} c_{\mathbf{k},j}^{\sigma} + Y \sum_{\mathbf{k},\mathbf{k}'} \sum_{\sigma} c_{\mathbf{k},i}^{\sigma\dagger} c_{\mathbf{k},j}^{\sigma} c_{\mathbf{k},j}^{\sigma} c_{\mathbf{k},i}^{\sigma} + W \sum_{\mathbf{k},\mathbf{k}'} \sum_{\sigma} c_{\mathbf{k},i}^{\sigma\dagger} c_{\mathbf{k},j}^{\sigma} c_{\mathbf{k},j}^{\sigma} c_{\mathbf{k},i}^{\sigma} \quad (5)$$

The first term in Eq. (5) is the direct IL hopping, while the second and third terms describe IL coupling in a general form. t is very small in oxide superconductors [10,14]. Y denotes the IL coupling assisted by direct Coulomb interaction between charged layers (this is of particular interest in our model). W is the coupling constant and can arise through the Coulomb interaction causing inter-band transitions at the Fermi surface to some of the occupied or empty bands away from the Fermi level, with finite dispersion, however, along the c -axis. In this paper we consider only the second term in Eq. (5) as the source of the attractive interaction for pairing and neglect the rest of the inter-layer Hamiltonian H_{ij}^{3D} ($t=0; W=0$).

We calculate then the energy of the nearly $2D$ electron pair condensate in the CuO_2 plane for the bilayer supercell problem. It is assumed that the pair condensate behaves as a nearly free electron gas with ab kinetic energy T_{kin}^{ab} and potential energy, which is mainly its in-plane self-electrostatic energy (E_c^{ab}) and the out-of-plane inter-layer interaction energy E_c^{IL} . For simplicity, the rest of the electron system is neglected completely. The external potential of the condensate is also excluded in this model, that is the lattice-condensate interaction, which is assumed to be negligible in the charged $(\text{CuO}_2)^2$ system (at least its contribution is negligible to the condensation energy). In other words the ionic background of the $(\text{CuO}_2)^2$ plane. The kinetic energy of the charge condensate is due to the hopping of the charge carriers between the CuO_2 sites within the sheets. We do not take into account the complications due to ionic heterogeneity, nonpointlike polarization, etc. The effective Coulomb interaction between spinless point-charges may be approximated by the expression $V_{eff}(r) = e^2 / (4\epsilon_0 \epsilon_c r)$, where ϵ_c takes into account phenomenologically the dielectric screening effect of the IL dielectric medium and confined hole charge. This kind of a rough approximation has widely used by several groups in the last decade

[13,39,47,70]. The important feature is that the c -axis dielectric screening (ϵ_c) is nearly reduced to the static value of the average background dielectric constant in the SC state. In accordance with this a sharp temperature dependence of $\epsilon_c(T)$ is found in BSCCO by c -axis optical measurements at T_c [35]. The static out-of-plane dielectric function can be obtained from the sum rule

$$\epsilon_c = \epsilon_c(0) + \frac{2}{\pi} \int_0^\infty \frac{\omega'^2 \epsilon''(\omega')}{\omega'^2 - \omega^2} d\omega'; \quad (6)$$

where $\epsilon''(\omega')$ is the dynamic component of $\epsilon_c(\omega')$ [68].

Although, the r -dependence of the screened in-plane electrostatic interaction between the condensed charges q_i and q_j is not perfectly $1/r$, we approximate it with the expression $V_{eff}^{ab} = e^2/4\epsilon_{ab}r$ as well, where screening is taken into account implicitly via ϵ_{ab} . The lowest eigenvalue of H given in Eq. (3) is $E = \hbar^2 k^2/2m$, where $(r_1; r_2) = \sum_{\mathbf{k}} g(\mathbf{k}) e^{i\mathbf{k} \cdot \mathbf{r}_1} e^{i\mathbf{k} \cdot \mathbf{r}_2}$ being the wavefunction of the interacting pair and $g(\mathbf{k})$ is a pair-correlation function [19]. Then the energy of the lowest eigenstate of the condensate in the SC state is approximated by using a pure dielectric form for the potential energy

$$E_{tot} = T_{kin}^{ab} + E_c^{ab} + E_c^{IL} = \frac{\hbar^2}{2m} (r_1; r_2) + \frac{e^2}{4\epsilon_{ab}} \sum_{i,j} \frac{q_i^{(1)} q_j^{(1)}}{r_{ij}^{(1)}} + \frac{1}{c} \sum_{n=1}^N \sum_{m=2}^N \sum_{i,j} \frac{q_i^{(n)} q_j^{(m)}}{r_{ij}^{(nm)}}; \quad (7)$$

where \hbar is the Planck constant, $m = 4m_e$ is the effective mass for the holes induced in the half-filled bands [47], n, m are layer indices, $r_{ij}^{(1)}$ and $r_{ij}^{(nm)}$ are the intra-layer and inter-layer point charge distances, respectively. The most important components are the interactions with $r_{ij}^{(1,2)}$ (bilayer components), however one has to sum up for the IL interactions with terms $r_{ij}^{(nm)}$, where $m = [2; 1]$. Note that only the interactions of various layers with the basal bilayer (FIG. 2) are considered along the c -axis in both directions (up and down). The in-plane electrostatic screening ϵ_{ab} is completely separated from the out-of-plane dielectric screening (ϵ_c). q_i, q_j are the partial point charges/atoms in the $N \times N$ superlattice model at optimal doping.

$$q_{i,j} = \frac{4e}{3N^2}; \quad (8)$$

The factor 3 is included in the denominator because each CuO_2 site consists of 3 atoms ($q_{i,j} = 0.53e$ at optimal charge separation, $N = 5$). For the sake of simplicity it is assumed that the charges are equally distributed among Cu and O atoms within a CuO_2 site. The number of the lattice sites in the characteristic superlattice is N^2 and

$$\epsilon_{ab} = (N - 1)a_0 \quad (9)$$

where $a_0 = 3.8\text{\AA}$ is the ab lattice constant. Note that the coherence length ξ_{ab} can be given in a_0 unit and the real space period N can be compared with ξ_{ab} via Eq. (9) (see also Fig. (1)). $N_h = 2e$ is the charge of the electron pair. The anti-hole charges q_i^{hole} must satisfy the charge sum rule within a characteristic bilayer over a coherence area ξ_{ab}^2

$$\sum_{i=1}^{N^2} q_i^{\text{hole}} = 4e; \quad (10)$$

where q_i^{hole} represents the anti-hole point charges. Naturally the charge neutrality $\sum_{i,j}^{N^2} (q_i^{\text{hole}} + q_j^{\text{hole}}) = 0$ is also required. In this paper we study the lattice size $N \times N = 5$, which we found nearly optimal for a variety of cuprates. However, it can be interesting to study the variation of the "characteristic" lattice size in different cuprates as a function of various parameters (doping, pressure etc.). The kinetic energy of the boson condensate arises from the hopping of anti-holes (hole-anti-hole exchange) between the adjacent sites within the sheets, against the electrostatic background of the rest of the hole-anti-hole system. Single hole-anti-hole exchange is forbidden since extraordinary repulsion occurs which leads to the redistribution of the entire hole-anti-hole charge pattern. The collective intersite anti-hole hopping results in the kinetic energy of the condensate.

V. THE CONDENSATION ENERGY IN THE CHARGE ORDERED BILAYER SUPERLATTICE MODEL

Important consequence of the model outlined in this paper is that the condensation energy (U_0) of the SC state can be calculated. We will show here that within our model the primary source of U_0 is the net energy gain in IL Coulomb energy occurs due to the asymmetrical distribution of the condensed hole-charge in the adjacent layers (see Fig. 2) below T_c .

Per definition U_0 is the free energy difference of the normal state and the superconducting state [10]. Therefore, taking the energy difference $U_0 = E_{tot}^{NS} - E_{tot}^{SC}$ using Eq. (7) we get

$$U_0 = E_c^{ab} + E_c^{IL}; \quad (11)$$

The ab -plane contribution to the SC condensation energy E_c^{ab} is expected to be negligible at optimal doping. That is because our Coulomb energy calculations indicate that the ab -plane Coulomb energy in the NS and in the SC state is nearly equal and therefore $E_c^{ab} \approx 0$ and also the kinetic energy of the pair-condensate E_{kin}^{ab} is much smaller by several order of magnitude than IL coupling. For instance we get for the prototypical 5×5 lattice 1.2×10^{-20} J ab -Coulomb energy both for the NS and for the SC COS. The COS of the NS is the one

given in Fig (3). The calculated ab-kinetic energy of the 5 × 5 condensate is 1.1×10^{-29} J if we use the very simple formula ("electron in a box")

$$T_{\text{kin}}^{\text{ab}} = \frac{\hbar^2}{2m} \frac{2e}{a_{\text{ab}} c}; \quad (12)$$

where c is the c-axis coherence length. The inter-layer Coulomb interaction (attraction) $E_c^{\text{IL}} = 1.3 \times 10^{-21}$ J for the 5 × 5 bilayer. It must be emphasized, however, that away from optimal doping the Coulomb energy of the condensate might affect the magnitude of the condensation energy. The abrupt jump of the measured condensation energy U_0 seen in the slightly overdoped regime [56] can be attributed to the increased E_c^{ab} contribution to U_0 .

In this article we restrict our study, however, to optimal doping and the study of the doping dependence of U_0 is planned in the near future. The main contribution to U_0 is then the IL energy gain E_c^{IL} in the SC state can be given as follows,

$$U_0 = E_c^{\text{IL;NS}} - E_c^{\text{IL;SC}}; \quad (13)$$

We can further simplify Eq. (13) if the NS contribution to Eq. (13) is $E_c^{\text{IL;NS}} = 0$, which holds if IL coupling is screened effectively in the NS (large density of the hole content in the IL space, large c (NS)). Again, if we assume $c = 33$, we get $E_c^{\text{IL;NS}} = 2 \times 10^{-18}$ J (12.3 eV) for a charge ordered 5 × 5 lattice which would be an extraordinarily large value for the IL Coulomb repulsion. Assuming, however, $c = 10000$, we get the more realistic Coulomb repulsion of $E_c^{\text{IL;NS}} = 10^{-22}$ J. Indeed there are measurements for cuprates which indicate large c in the NS in the range of 10^3 to 10^5 [63]. Extraordinarily large dielectric constant has also been found recently in perovskite materials [36]. Anyhow the "relaxation" of the huge IL Coulomb repulsion in hole-doped cuprates in the NS can not easily be understood without the consideration of a large c . Nevertheless experimental measurements and theoretical speculations suggest that c in cuprates and in other materials with perovskite structure is strongly temperature and doping dependent [35]. The sharp decrease of c below T_c should also be explained within our bilayer model by the pair-condensation of the hole-content to the sheets. This is what can be seen in the c-axis optical spectra of cuprates [23,60]. The lack of the c-axis plasma edge in the NS is an obvious experimental evidence of the strong temperature dependence of c . Then we have

$$2(n+1)N^2U_0 = E_c^{\text{IL;SC}}; \quad (14)$$

where $E_c^{\text{IL;SC}}$ is the Coulomb energy gain in the SC state. U_0 is the experimental condensation energy given per unit cell. Eq. (14) is generalized for multilayer cuprates introducing n , the number of CuO_2 layers within a multilayer block.

The hole-conductivity in the SC state is strictly 2D phenomenon, no direct IL hopping of quasiparticles is considered within this model. T_c is mainly determined by the inter-plane distance and by the static c-axis dielectric constant (the c-axis component of the dielectric tensor). An interesting feature of the NN bilayer model is then that it is capable of retaining the 2D character of superconductivity while T_c is enhanced by 3D Coulomb interactions.

VI. THE CONDENSATION ENERGY AND T_c

There are number of evidences are available which suggest that HTSC occurs beyond the BCS limit. In those materials which contain nearly isolated single layers, such as $\text{Bi}_2\text{Ba}_2\text{CuO}_{6+x}$ ($T_c = 20$ K [69]) or superlattice structures (periodically layered materials) such as O-doped $(\text{BaCuO}_2)_2 = (\text{CaCuO}_2)_n$ thin films, when $n = 1$ [6] and in $\text{YBa}_2\text{Cu}_3\text{O}_{7-x}$ \rightarrow $\text{PrBa}_2\text{Cu}_3\text{O}_7$ (YBCO/PBCO) [3,5,7] the critical temperature is limited to $T_c = 30$ K (below the BCS limit), therefore these materials are not considered as high- T_c superconductors in this article. In these compounds the IL distance is so large that the CuO_2 planes are decoupled and the superconducting properties can be understood within the BCS formalism. However, the multilayer Bi-compounds (with the same charge reservoir as in the single layer Bi2201), the $(\text{BaCuO}_2)_2 = (\text{CaCuO}_2)_n$ thin films, when $n = 2$ [6] or YBCO with thin $\text{PrBa}_2\text{Cu}_3\text{O}_7$ layer [3,5,7] exhibit HTSC. Therefore it is worth to explain the enhancement of T_c beyond the BCS limit assuming other mechanism than the electron-phonon coupling. Inter-layer Coulomb coupling can be a natural source of the condensation energy and of HTSC. Checkerboard-like charge pattern (COS) seen experimentally [41-43] directly leads to IL energy gain and to potential energy driven condensation energy if the hole-anti hole charge pattern is asymmetrically condensed to the adjacent layers (Fig 2). Assuming that thermal equilibrium occurs at T_c for the competing charge ordered phases of the NS and the SC state the following equation for the condensation energy can be formulated using Eq. (14),

$$2(n+1)N^2U_0 = 2(n+1) \frac{ab}{a_0} + 1 U_0 = k_B T_c; \quad (15)$$

At a first look this formula seems to be unusual because of the dependence of the condensation energy on T_c . The available measurements of the condensation energy on various cuprates show no correlation of U_0 with the critical temperature.

One of the important goals of this paper, however, to show that correlation can indeed be found with T_c if T_c is plotted against $2N^2U_0$ (the bilayer condensation energy). In other words the condensation energy of the coherence bilayer-hole system shows correlation with T_c . In order to test the validity of Eq. (15) we estimate the coherence

TABLE I. The calculated coherence length of the pair condensate using the experimental condensation energies of various cuprates and Eq. (16) at optimal doping.

| | T_c (K) | $k_B T_c$ (meV) | U_0 (eV/u.c.) | ξ_{ab}^{calc} (a_0) | ξ_{ab}^{exp} (a_0) |
|--------|-----------|-----------------|------------------|-----------------------------|----------------------------|
| LSCO | 39 | 2.5 | 21 ^a | 7 | 5 ^h |
| Tl2201 | 85 | 7 | 100 ^b | 5 | |
| Hg1201 | 95 | 7.8 | 80 ^c | 5 | 5 ^c |
| YBCO | 92 | 7.5 | 110 ^d | 3 | 4 ^g |
| Bi2212 | 89 | 7.3 | 107 ^e | 4 | 5 ^f |

U_0 is the measured condensation energy of various cuprates in eV per unit cell at optimal doping. ^a $U_0 = 2$ J/mol from [52,53], ^b [18], ^c $U_0 = 12$ J/mol from [54,67] and ^d $U_0 = 11$ J/mol from [48,56,57], ^e $U_0 = 10$ J/mol from [51], ^f from recent measurements of Wang et al. [20], ^g from [19,49], ^h from [9], ξ_{ab}^{calc} is calculated according to Eq. (16) and is also given in Table I and ξ_{ab}^{exp} is the measured in-plane coherence length given in a_0 [39]. The notations are as follows for the compounds: LSCO ($La_{1.85}Sr_{0.15}CuO_4$), Tl2201 ($Tl_2Ba_2CuO_6$), Hg1201 ($HgBa_2CuO_{4+}$), YBCO (YBa_2CuO_7) and Bi2212 is $Bi_2Sr_2CaCu_2O_{8+}$.

length of the pair condensate using Eqs. (15) and (9) using only experimental data,

$$\xi_{ab} = \frac{2(n+1)U_0}{k_B T_c} \quad (16)$$

The results are given in Table I as ξ_{ab}^{calc} and compared with the available measured ξ_{ab}^{exp} . The agreement is excellent which strongly suggests that Eq. (16) should also work for other cuprates. The validity of Eq. (15) is clearly clarified in FIG 4 using mostly experimental information for ξ_{ab} , T_c and U_0 (values are given in Table I). For Tl2201 no measured ξ_{ab} is found in the literature, therefore the estimated ξ_{ab} is used (given in Table I). In Section VII we will show that using this estimated value of $N = 6$ we predict ξ_c in nice agreement with optical measurements for Tl2201. Remarkable feature of FIG 4 is that the slope of the linear fit to the measured data points precisely gives us k_B which nicely confirms Eq. (15). The underlying physics of HTSC seems to be reflected by Eq. (15): the equation couples the observable quantities T_c , U_0 and ξ_{ab} . We predict for the multilayer Hg-cuprates, Hg1212 ($T_c = 126$ K) and Hg1223 ($T_c = 135$ K) the condensation energies 146 and 117 eV/u.c. ($\xi_{ab} = 4a_0$ [55]), respectively using Eq. (15).

Furthermore, we find correlation between the condensation energy U_0 and N : the larger U_0 is connected with smaller N (see also FIG 5). The stronger localization of the pair-condensate wave function seems to lead to larger IL condensation energy and hence to larger T_c . This is again an unexpected result, since the stronger localization of the Cooper pairs should increase the Coulomb self-repulsion of the condensate and hence should suppress T_c . Note, however, that within a liquid-crystal-like COS the self-repulsion problem is not crucial. The hole-

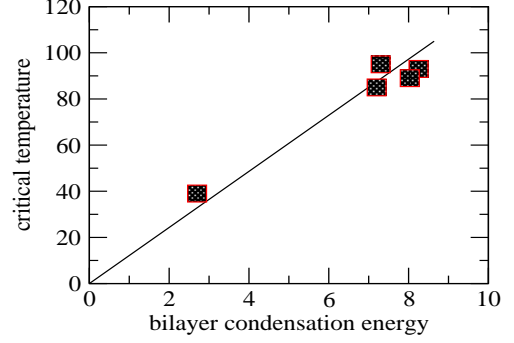


FIG. 4. The critical temperature (K) at optimal doping as a function of the bilayer condensation energy ($2(n+1)N^2U_0$, meV) using Eq. (15). The real space period N is directly related to ξ_{ab} via Eq. (9). The straight line is a linear fit to the data. The slope of the linear fit is k_B which is a strong evidence of Eq. (15).

anti-hole Coulomb interactions are attractive, although cancelled by the intra-hole and intra-anti-hole repulsions (intra CuO_2 site repulsion,).

Interestingly the most localized coherence area ($4a_0$) is provided by YBCO which is the less anisotropic material among HTSC cuprates (the resistivity ratio $\rho_{ab}/\rho_c = 200$ [3]). The more anisotropic Hg1201 gives us somewhat weaker localization of the condensate wave-pocket for similar T_c . The comparison between various materials, however, is much more complicated. In general we can say that T_c is a function of the following parameters considered in this study: N , p , the IL distance d and ϵ_c . In section VII we further analyse this complex behaviour of T_c focusing on the calculated IL dielectric constant ϵ_c . The estimated ξ_{ab} values given in Tables I and II of the bilayer COS are in close agreement with the experimental coherence areas ξ_{ab} which supports the validity of our basic Eq. (15).

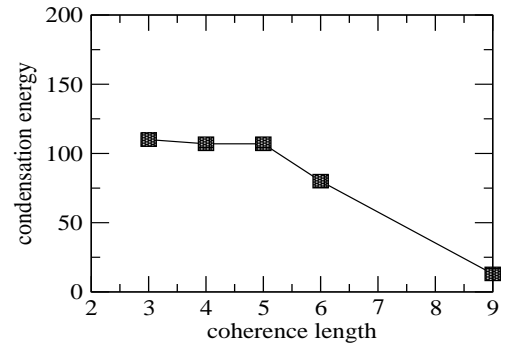


FIG. 5. The measured condensation energy (given in Table I, eV/u.c.) as a function of the calculated coherence length (a_0) using Eq. (16).

The expression Eq. (15) leads to the very simple formula for the critical temperature

$$T_c(N; d; q; d_c) = \frac{e^2}{4\epsilon_0\epsilon_c k_B} \sum_{n=1}^{N-1} \sum_{m=2}^N \frac{q_i^{(n)} q_j^{(m)}}{r_{ij}^{(n,m)}} \quad (17)$$

where N_1 is the number of layers along the c-axis. When $N_1 \rightarrow 1$, bulk T_c is calculated. T_c can also be calculated for thin films when N_1 is finite and ϵ_c can also be derived

$$\epsilon_c = \frac{e^2}{4\epsilon_0 k_B T_c} \sum_{n=1}^{N-1} \sum_{m=2}^N \frac{q_i^{(n)} q_j^{(m)}}{r_{ij}^{(n,m)}} \quad (18)$$

where a c-axis average of ϵ_c is computed when $N_1 \rightarrow 1$.

The calculation of the c-axis dielectric constants ϵ_c might provide further evidences for Eq. (15) when compared with the measured values [35,61,70]. In Table II we have calculated the static dielectric function ϵ_c using Eq. (18) and compared with the experimental impedance measurements [64]. ϵ_c can also be extracted from the c-axis optical measurements using the relation [18,48]

$$\epsilon_c = \frac{c}{v_p}; \quad (19)$$

where c/v_p and ϵ_c are the speed of light, c-axis plasma frequency and the c-axis penetration depth. The general conclusion can be drawn on the basis of the data depicted in Table II that the ϵ_c values obtained from c-axis optical measurements are somewhat smaller than the values obtained from impedance measurements [64]. The reason for this is not clear. Our calculations support the optical measurements vs. the impedance experiments if ϵ_c is calculated at the experimental coherence length.

For the prototypical cuprate LSCO we get the value of $\epsilon_c = 27.3$ which is comparable with the experimental value of 23 [61] using $N = 7$ which corresponds to $6a_0$ (23.4 Å ($a_b = 20-30$ Å [79])). The overall good agreement of the calculated ϵ_c with the measurements is due to our finding that the IL charging energy is surprisingly in the range of $k_B T_c$ when the real space period N (coherence length) is reasonably chosen.

Not useless to note again the correlation in Table I. between a_b and U_0 . There seems to be a correlation between the real-space localization of the Cooper wavefunction and the SC energy gain U_0 .

The real-space "shrinking" of the Cooper wavefunction must directly be related to the enhancement of pairing. Within our model the primary source of increased pairing is the IL energy gain (Coulomb induced pairing).

Optimally doped YBCO/PBCO with decoupled layers shows no HTSC ($T_c = 20$ K) indicating that optimal carrier concentration within isolated layers leads to

TABLE II. The calculated dielectric constant ϵ_c using Eq. (18) in various cuprates as a function of the coherence length a_b of the charge ordered state.

| | d (Å) | T_c (K) | a_{ab}^{calc} (a_0) | ϵ_c | ϵ_c^{exp} |
|---------------------------------|------------------|-----------|---------------------------|--------------|-------------------------------------|
| CaCuO ₂ ^b | 4.64 | 110 | 4 | 80.8 | |
| CaCuO ₂ | 3.19 | 89 | 7 | 83.5 | |
| LSCO | 6.65 | 39 | 5 | 27.9 | 23 |
| | | | 6 | 27.3 | 3;13.5 ^c |
| | | | 7 | 11.3 | |
| Hg1201 | 9.5 | 95 | 5 | 33.5 | 34 ^d |
| Hg- (10 GPa) | 8.5 | 105 | 4 | 27.6 | |
| Hg- (20 GPa) | 8.2 | 120 | 4 | 25.0 | |
| Tl2201 | 11.6 | 85 | 3 | 8.7 | 11.3 ^e |
| | | | 4 | 26.8 | |
| | | | 5 | 13.0 | |
| | | | 6 | 8.0 | |
| Bi2201 | 12.2 | 20 | 3 | 32.6 | 40 ^g |
| | | | 4 | 110.8 | |
| | | | 5 | 10.1 | |
| YBCO | 8.5 ^h | 93 | 3 | 19.4 | 34 ^f ; 23.6 ^j |
| | | | 4 | 31.1 | |

where a_{ab}^{calc} is the estimated in-plane coherence length given in $a_0 = 3.9$ Å. The estimated a_{ab}^{calc} is that value which is associated with that calculated ϵ_c which is in good agreement with the experimental ϵ_c . the bold faced values are those which account the best for comparison with experiment and are in accordance with the results of Table I. d is the CuO₂ plane to plane inter-layer distance in Å [13], T_c is the experimental critical temperature. ϵ_c is from Eq. (18). ^b Ca_{0.3}Sr_{0.7}CuO₂ [66], ^c [61], or from reactivity measurements using Eq. (19), $v_p = 55$ cm⁻¹ [81], $\epsilon_c = 3$ m [67], ^d experimental ϵ_c^{exp} values are taken from Am. Inst. of Phys. Handbook, McGraw-Hill, Ed. D, E. Gray (1982), the ϵ_c value of the ionic-background (Hg1201: BaO), The pressure dependent T_c values and IL distance data are taken from [71,76], ^e from [18], ^g from [35], ^h for YBCO the reduced IL d = 8.5 Å is used instead of the c-axis lattice constant (inter-bilayer block distance), ^f from [70], ^j from reactivity measurements: $v_p = 60$ cm⁻¹ [81], $\epsilon_c = 0.9$ m [37], ϵ_c can be deduced using Eq. (19).

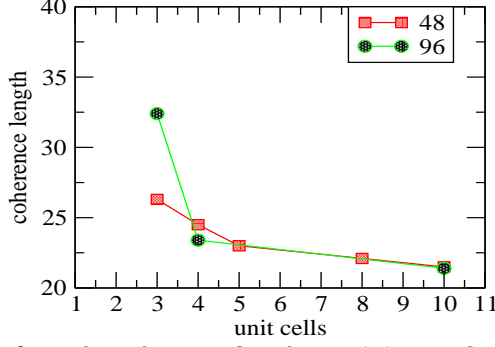


FIG. 6. The coherence length λ_{ab} (Å) as a function of the YBCO thickness (in unit cells) at fixed thickness of the barrier (insulating) layer PBCO (48 and 96 Å) reproduced from Table II. of ref. [73].

probably BCS superconductivity with low critical temperature. Setting in IL coupling (decreasing the thickness of the PBCO phase) T_c is enhanced due to the increase of IL coupling [3,5]. Further experimental studies on artificially layered materials, such as the measurement of λ_{ab} as a function of the thickness of the insulating phase PBCO should explain the importance of IL coupling in cuprates. The considerable increase in λ_{ab} as a function of IL decoupling (increase in PBCO thickness or decrease in YBCO thickness) would be a strong evidence for the model presented in sections III-V. Looking for such an article in the literature an interesting publication is found which reveals our expectation [73]. The extensive measurements of the upper critical field in $(YBCO/PBCO)_n$ superlattices indeed results in the increase of λ_{ab} as a function of decreased thickness of YBCO layers. λ_{ab} varies from $4.5a_0$ up to $8a_0$ when the thickness of the YBCO phase is decreased from 10 unit cells to 3. Unfortunately this article contains no measurements for 1–2 unit cell thick samples. In FIG 6 we give the measured coherence length in YBCO/PBCO getting the data from ref. [73]. We predict the rapid increase of λ_{ab} for dielectrically isolated single layers of YBCO for one or two-unit-cell thick samples which is the remnant of purely BCS features. These striking results represent a strong evidence for the correlation between IL coupling and the coherence length λ_{ab} which is predicted by the model presented here. Strikingly, the contraction of the Cooper wave-function (the strengthening of pairing) is strongly coupled to the enhancement of IL Coulomb coupling.

VIII. MULTILAYER AND PRESSURE EFFECTS

Multilayer and pressure effects on T_c can also be discussed in terms of in-plane and out-of-plane localization of the hole charge. In multilayer systems E_c^{IL} is composed of intra- and inter-block contributions. We use

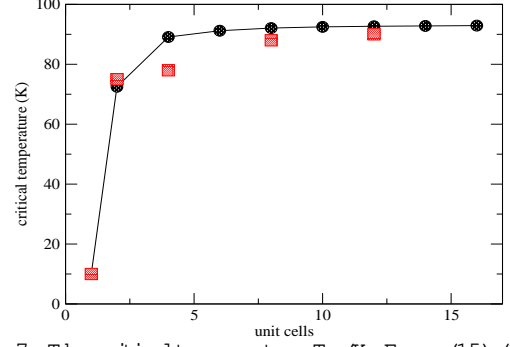


FIG. 7. The critical temperature T_c (K, Eqs. (15)–(18)) vs. the number of unit cells along the c-axis in YBCO using the 4–4 model. Circles and squares correspond to the calculated and experimental values [5].

the notation block for the multilayer parts $CaCu_2O_4$, $Ca_2Cu_3O_6$, etc. Eq. (14) can then be modified for multilayer cuprates as follows,

$$U_0 = E_c^{IL; intra} + E_c^{IL; inter}; \quad (20)$$

where

$$E_c^{IL; intra} = (l-1)E_c^{IL}(d_{intra}; intra); \quad (21)$$

l denotes the number of layers. Therefore, intra-block charging energy further enhances T_c on top of the corresponding single-layer inter-block value. YBCO is a peculiar example of cuprates in which HTSC is purely coming from inter-block coupling as it was explained on the basis of $YBa_2Cu_3O_{7-x}/PbBa_2Cu_3O_{7-x}$ superlattice structures [3]. In YBCO the $Y(CuO_2)_2$ bilayer alone does not show HTSC when isolated from each other in artificially layered materials ($T_c \approx 20K$). The dependence of T_c in YBCO on the number of unit cells along the c-axis is calculated using Eq. (17) and the results are depicted on FIG 7. The experimental points [5] are relatively well reproduced indicating that 5 unit cell thick thin film is already the remnant of the bulk properties of cuprates.

It is worth mentioning the intercalation experiment on Bi2212 [4]. Intercalation of I or organic molecules into the $(BiO)_2(SrO)_2$ layers of Bi2212 results in no significant change in T_c . Basically inter-layer intercalation is introduced to reduce interlayer coupling (test of inter-layer theory, ILT) and to enhance anisotropy in SC properties. Using MBE deposition technique, ultrathin films of Bi-Sr-Ca-Cu-O (Bi2212) have been synthesized [80]. The few-unit-cell-thick samples show HTSC similar to that of the bulk material independently of the film thickness. These results present great challenge to ILT [10] and support low-dimensional SC theories.

In the light of the NN model, however, it is not surprising that in Bi2212 the nearly isolated bilayers are superconductors. The single layer material Bi2201 ($Bi_2Sr_2CuO_6$) gives very low T_c ($\approx 20K$) [69], which

indicates that the dielectrics $(\text{BiO})_2(\text{SrO})_2$ strongly reduces IL coupling, indeed the estimated ϵ_c is quite large (Table II) which is attributed to the weakly interacting $(\text{BiO})_2$ bilayer (the $\text{BiO}-\text{BiO}$ distance is 3.7\AA [4]). Dielectric constant measurements [59] and the obtained small plasma frequency using c-axis optical measurements ($\sim 5\text{cm}^{-1}$) [61] in Bi-compounds also provide relatively large dielectric constants in accordance with our calculations. The extremely large conduction anisotropy $\sim 10^6$ found in Bi-based cuprates also supports these findings [3]. Nearest-neighbouring Cu-O planes in Bi-compounds are nearly insulated [70]. Therefore, in the multilayer Bi-compounds bilayer and trilayer blocks are responsible for the high- T_c , inter-block coupling is negligible. The multilayer Bi-compounds provide then an example for pure intra-block HTSC. In these materials the multilayer-blocks are dielectrically isolated. However, in the most of the cuprates T_c is enhanced both via intra- and inter-block effects. An important consequence of the bilayer $N \times N$ model is that isolated single layers do not show HTSC, coupling to next-nearest CuO_2 plane is essential in HTSC. It is possible then to estimate ϵ_c for the bilayer block, since $E_c^{\text{IL};\text{inter}} \rightarrow 0$ in the Bi-compounds in Eq. (20). In the hypothetical bilayer system in Table II ($\text{Ca}(\text{CuO}_2)_2$; $d = 3.19\text{\AA}$; $T_c = 89\text{K}$), which is the building block of bilayer cuprates, we find the value of $N = 8$ accounting for realistic ϵ_c . $N = 8$ is in accordance with the measured relatively "large" coherence length of $a_{\text{ab}} \sim 27\text{\AA}$ ($(N-1)a_0 = 7a_0 \sim 27.3\text{\AA}$) [77].

Also, upon pressure (p) the inter-layer spacing decreases, which increases E_c^{IL} without the increase of the hole content. Saturation of $T_c(p)$ is reached simply when increasing IL steric repulsion starts to destabilize the system. In systems, such as YBCO or LSCO, negative or no pressure dependence of T_c is found [3] due to the short Cu-O apical distance ($d_{\text{CuO}} \sim 2.4\text{\AA}$) which leads to already steric repulsion at ambient pressure and to the weakening of HTSC. In these systems the net gain in charging energy is not enough to overcome steric repulsions at high pressures. We give the calculated ϵ_c values in Hg1201 for high pressures in Table I. ϵ_c does not depend on the pressure and therefore the pressure dependence of T_c can be given by Eq. (17).

With these results, we are now in a position to reach the conclusion that the $N \times N$ model can readily account for at least certain physical properties of multilayer cuprates, such as pressure, doping and multilayer dependence of T_c . Furthermore it is possible to make some estimations on the upper limit of T_c using Eq. (17) for T_c . Assuming relatively small $\epsilon_c \sim 10$ and short inter-layer spacing $d \sim 7\text{\AA}$ we get the value of $T_c \sim 333\text{K}$ for a strongly localized electron pair with 5×5 coherence area. Of course, we have no clear cut knowledge at this moment on how the pair condensate wave-function spreads upon varying ϵ_c and d . Effective localization of the Cooper-pair wave-pocket could lead, however, to room temperature superconductivity under proper structural and dielec-

tric conditions if the model presented above is applicable.

According to the stripe scenario, the charge ordered state of the coherence area can also be seen in many cuprates as one-dimensional stripe order or charge density waves [43]. The striped antiferromagnetic order found in LSCO by magnetic neutron scattering experiments [42] also implies a spin-density of periodicity $\sim 8a_0$ reminiscent of the coherence area. The incommensurate "checkerboard" patterns seen with a spatial periodicity of $\sim 8a_0$ in the vortex core of Bi2212 obtained by scanning tunneling microscopy [41] is also consistent with our $N \times N$ hole-anti-hole charge ordered state where $N = 8$ to 9 in BSSCO.

IX. CONCLUSION

In this paper we studied the pair condensation and content of the hole-content on a CuO_2 superlattice layer as a function of inter-layer distance and dielectric permittivity of the charge reservoir.

The assumption of a 2D, 3D quantum phase transition of the hole-content at T_c in HTSC materials is thought to be an important general feature of pair-condensation and is supported by c-axis optical measurements and by first-principles calculations. Our proposal is that the c-axis charge dynamics of the hole-content contributes significantly to the condensation energy below T_c . We find that the inter-layer capacitance is temperature dependent in cuprates and therefore the drop of the c-axis dielectric constant can be seen below T_c . This is what leads to then the stabilization of the superconducting state vs. the normal state.

We have found that a pair condensate can be distributed on a $N \times N$ square lattice layer in such a way that the lattice sites are filled by $q = 0.16e$ condensed charge alternatively depending on the hole(+ q)-anti-hole($-q$) charge separation dq . In this way a charge ordered state of the pair-condensate occurs with a "checkerboard" like pattern seen recently by experiment [41]. The phase separation of hole-electron pairs (hole-anti-hole pairs) in this model is stabilized electrostatically. The maximum charge separation is $dq = 0.32e$, if the optimal hole content $p_0 = 0.16e$.

In the adjacent layers the electron-hole pairs are distributed in such a way that complementary charge pattern occurs (inter-layer charge asymmetry) in order to maximize the inter-layer charging energy. A hole in one plane is neighbouring with an anti-hole in the other (see FIG 2.). In this way we derived a charge ordered $N \times N$ correlated bilayer supercell model of the superconducting state with inter-layer charge antisymmetry which directly leads to inter-layer Coulomb energy gain in

the superconducting state. The IL charge asymmetry could directly be tested experimentally using e.g. two-cell-thick thin SC films, and the "checker-board" STM images of both sides of the thin film could be measured. A complementary "checker-board" charge pattern would reveal our finding.

The superlattice nature of the pair condensate is directly related to the smallest size of the condensate wave-pocket which is remarkably comparable with the measured in-plane coherence length of $\xi_{ab} = 10-20a_0$ ($4a_0-15.6a_0$) of single cuprates, where $a_0 = 3.8\text{\AA}$ is the in-plane lattice constant. The coherence area of the Cooper-pair wave-function in cuprates is strongly localized, which is due to inter-layer charging effects.

The bilayer model with 4e boson charge naturally implies the mass enhancement of $m^* = 4m_e$ in accordance with measurements. The calculated inter-layer charging energy is in the range of the experimental condensation energy for the bilayer-hole system.

The static dielectric constant ϵ_c is calculated for a couple of cuprates and compared with the available experimental measurements. The general agreement is quite good indicating that the pure inter-layer electrostatic model leads to proper description of the static dielectric response of these layered materials.

The basic microscopic mechanism of HTSC is to be understood within the BCS-Eliashberg theory. The limiting critical temperature for BCS-type superconductor is around 20K as it was found for cuprates with nearly isolated CuO_2 layers (BSCCO , YBCO/PBCO superlattices etc.). The detailed study of this model showed that the inter-layer charging energy is proportional to the thermal motion at T_c , if the c-axis dielectric constant ϵ_c and the coherence area is appropriately chosen. The correlation between the coherence area ξ_{ab} and inter-layer coupling is predicted by our model. The stronger IL coupling leads to smaller ξ_{ab} . This relation is evidenced by the measurements of ξ_{ab} in YBCO/PBCO films with varying YBCO thickness.

If the physical picture derived from our model is correct, it should be a guide for further experimental studies aiming to improve SC in cuprates or in other materials. This can be done by tuning the IL distance and ϵ_c (increasing the polarizability of the dielectric, hence decreasing ϵ_c) in these materials. The application of this model to other class of HTSC materials, such as fullerides or MgB_2 is expected to be also effective.

ACKNOWLEDGEMENT

It is a privilege to thank M. Menyhard for his continuous support. I greatly indebted to E. Sherman for reading the manuscript carefully and for the helpful informations. I would also like to thank for the helpful discussions with T. G. Kovacs. Special thank should also be given for plenty of technical help to A. Sulyok and to G. Tamás. This work is supported by the OTKA grant F037710 from the Hungarian Academy of Sciences

-
- [1] Q. Xiong, Y. Y. Xue, Y. Cao, F. Chen, Y. Y. Sun, J. Gibson, and C. W. Chu, *Phys. Rev. B* 50, 10346 (1994)
 - [2] J. E. Hirsch, *Science* 295, 2226. (2002)
 - [3] N. M. P. Lakda, *High-Temperature Superconductivity*, Springer, 1995
 - [4] J. Choy et al., *Science* 280, 1589. (1998), X.-D. Xiang, et al., *Nature* 348, 145. (1990)
 - [5] Q. Li, et al., *Phys. Rev. Lett.* 64, 3086. (1990)
 - [6] G. Balestrino et al., *Phys. Rev. B* 58, 8925. (1998)
 - [7] T. Terashima, et al., *Phys. Rev. Lett.* 67, 1362. (1991)
 - [8] G. Balestrino et al., *Phys. Rev. Lett.* 89, 156402-1 (2002)
 - [9] P. W. Anderson, *The Theory of Superconductivity in the High- T_c Cuprate Superconductors*, Princeton Univ. Press, 1997
 - [10] P. W. Anderson, *Physica C* 341-348, 9. (2000), cond-mat/0201429
 - [11] T. Schneider, cond-mat/0110173, T. Schneider, H. Keller, *Phys. Rev. Lett.* 86, 4899. (2001)
 - [12] J. M. Wheatley, T. C. Hsu, P. W. Anderson, *Nature* 333, 121. (1988)
 - [13] D. R. Harshman, A. P. Mills, *Phys. Rev. B* 45, 10684. (1992), and references therein
 - [14] Z. Tesanovic, *Phys. Rev. B* 36, 2364. (1987)
 - [15] A. K. Rajagopal, S. D. Mahanti, *Phys. Rev. B* 44, 10210. (1991), S. S. Jha, A. K. Rajagopal, *Phys. Rev. B* 55, 15248. (1997)
 - [16] X.-D. Xiang, et al., *Phys. Rev. Lett.* 68, 530. (1992)
 - [17] J. Ihm and B. D. Yu, *Phys. Rev. B* 39, 4760. (1989)
 - [18] A. A. Tsvetkov et al., *Nature*, 395, 360. (1998)
 - [19] M. Tinkham, *Introduction to Superconductivity*, McGraw-Hill, Inc. New York, 1996
 - [20] Y. Wang et al., *Science* 299, 86. (2003)
 - [21] J. B. Torrance et al., *Phys. Rev. Lett.* 61, 1127. (1988), H. Zhang and H. Sato, *Phys. Rev. Lett.* 70, 1697. (1993)
 - [22] J. L. Tallon, et al., *Phys. Rev. B* 51, 12911. (1995), P. Resland, et al., *Physica C* 165, 391. (1991)
 - [23] D. N. Basov et al., *Science* 283, 49. (1999)
 - [24] K. Tamasku, Y. Nakamura, S. Uchida, *Phys. Rev. Lett.* 69, 1455. (1992)
 - [25] S. Tajima, et al., *Phys. Rev. B* 48, 16164. (1993)
 - [26] A. S. Katz, et al., *Phys. Rev. B* 61, 5930. (2000)
 - [27] D. N. Basov, et al., *Phys. Rev. B* 63, 134514. (2001)

- [28] T. Motohashi, et al, Phys. Rev. B 61, 9269. (2000)
- [29] W. E. Pickett, Rev. Mod. Phys. 61, 433. (1989)
- [30] R. P. Gupta, M. Gupta, Phys. Rev. B 21, 15617. (1995)
- [31] C. Ambrosch-Draxl, P. Sule, H. Auer, E. Y. Shernan, (2003), in press in Phys. Rev. B, P. Sule, C. Ambrosch-Draxl, H. Auer, E. Y. Shernan, cond-mat/0109089,
- [32] Y. Ando, A. N. Lavrov, S. Komiyama, K. Segawa, X. F. Sun, cond-mat/0104163
- [33] K. Semba, A. Matsuda, Phys. Rev. Lett. 86, 496. (2001)
- [34] A. Yamamoto, W. Hu, S. Tajima, Phys. Rev. B 63, 24504. (2001)
- [35] H. Kitano, T. Hanaguri, A. Maeda, Phys. Rev. B 57, 10946. (1998),
- [36] C. C. Homes, et al, Science, 293, 673. (2001)
- [37] H. Kitano et al, Phys. Rev. B 51, 1401. (1995)
- [38] T. Fujii, et al, cond-mat/0205121, L. He, et al, cond-mat/0110166, W. Si, et al, cond-mat/0205153
- [39] R. Friedberg, H. S. Zhao, Phys. Rev. B 44, 2297. (1991), Phys. Rev. B 39, 11482. (1989)
- [40] M. Vojta, Y. Zhang, S. Sachdev, Phys. Rev. B 62, 6701. (2000)
- [41] J. E. Hoffman et al, Science 295, 466. (2002)
- [42] B. Lake, et al, Nature 415, 299. (2002)
- [43] C. Howald, et al, cond-mat/0208442
- [44] E. Dagotto, et al, cond-mat/0209689
- [45] M. Vojta, cond-mat/0204284
- [46] S. Stinzingen, Z. Zwebner, Phys. Rev. B 56, 9004. (1997)
- [47] M. DiStasio, K. A. Muller, L. Pietronero, Phys. Rev. Lett. 64, 2827. (1990), and references therein
- [48] P. W. Anderson, Science, 279, 1196. (1998)
- [49] U. Welp, et al, Phys. Rev. Lett. 62, 1908. (1989)
- [50] L. K. Musin-Eibaum et al, Phys. Rev. Lett. 62, 217. (1989)
- [51] J. L. Tallon et al, cond-mat/0211048,
- [52] J. W. Loram et al, J. Phys. Chem. Solids, 62, 59. (2001) and references therein
- [53] N. Momono et al, J. Phys. Soc. Jap. 71, 2832. (2002)
- [54] B. Billon et al, Phys. Rev. B 56, 10824. (1997)
- [55] J. R. Thompson, et al, Phys. Rev. B 54, 7505. (1996)
- [56] J. L. Tallon et al, Physica Status Solidi B 215, 531. (1999)
- [57] J. L. Tallon and J. W. Loram, Physica C 349, 53. (2001)
- [58] C. Kittel, Quantum Theory of Solids, Wiley & Sons, New York, (1987)
- [59] K. B. R. Varma, et al, Appl. Phys. Lett. 55, 75. (1989)
- [60] H. J. A. M. Olegraaf, C. Presura, D. van der Marel, P. H. Kes, M. Li, Science 295, 2239. (2002), D. van der Marel, A. Tsvetkov, M. Grueninger, H. J. A. M. Olegraaf, Physica C 341-348, 1531. (2000)
- [61] D. Reagor et al, Phys. Rev. Lett. 62, 2048., (1989)
- [62] J. E. Hirsch, Physica C 199, 305. (1992)
- [63] G. Cao et al, Phys. Rev. B 47, 11510. (1993), G. P. Mazza, et al, Phys. Rev. B 47, 8119. (1993), C. M. Rey, et al, Phys. Rev. B 45, 10639. (1990)
- [64] T. Takayanagi, M. Kogure, I. Terasaki, cond-mat/0108483, and references therein, I. Terasaki, T. Mizuno, K. Inagaki, Y. Yoshino, cond-mat/0204537
- [65] R. M. Hazen, Crystal Structures of High Temperature Superconductors, in Physical Properties of High Temperature Superconductors, Ed. D. M. Ginsberg, (1990)
- [66] M. Azuma et al, Nature (London) 356, 775. (1992)
- [67] J. R. Kirtley, et al, Phys. Rev. Lett. 81, 2140. (1998)
- [68] P. Nozières, D. Pines, The Theory of Quantum Liquids, Perseus Books, 1999
- [69] Z. Konstantinovic, et al, Phys. Rev. B 66, 20503. (2002)
- [70] D. Ariosa, H. Beck, Phys. Rev. B 43, 344. (1991)
- [71] D. L. Novikov et al, Phys. Rev. B 54, 1313. (1996)
- [72] T. Timusk, B. Statt, Rep. Prog. Phys. 62, 91. (1999)
- [73] H. C. Yang, L. M. Wang, H. E. Homg, Phys. Rev. B 59, 8956. (1999)
- [74] K. C. Hewitt, J. C. Irwin, Phys. Rev. B 66, 054516, (2002), cond-mat/0012413
- [75] C. Panagopoulos, T. Xiang, Phys. Rev. Lett. 81, 2336. (1998)
- [76] L. Gao, et al, Phys. Rev. B 50, 4260. (1994)
- [77] I. Matsubara, et al, Phys. Rev. B 45, 7414. (1992)
- [78] R. Kleiner, et al, Phys. Rev. Lett. 68, 2394. (1992)
- [79] See e.g. Physical Properties of High Temperature Superconductors, Ed. D. M. Ginsberg, (1989)
- [80] K. Saito, M. Kaise, Phys. Rev. B 57, 11786. (1998)
- [81] S. DasSarma, E. H. Hwang, Phys. Rev. Lett. 80, 4753. (1998)